Direct measurements of fusion reactions (with heavy ions) of astrophysics impact

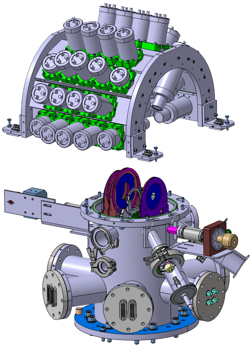

Marcel Heine for the STELLA Collaboration

IPHC/CNRS Strasbourg

February 16, 2025

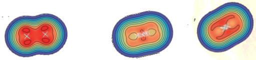

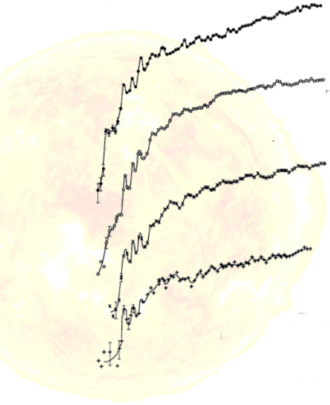

Heavy ion reactions during carbon burning in massive stars

- $M \geq 7.5 \ldots 9.5\ M_{\odot}$
- core made of oxygen and carbon
- Coulomb well

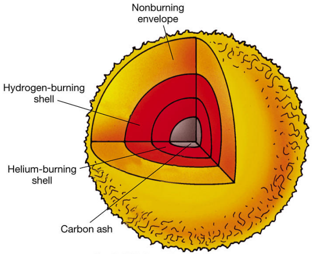

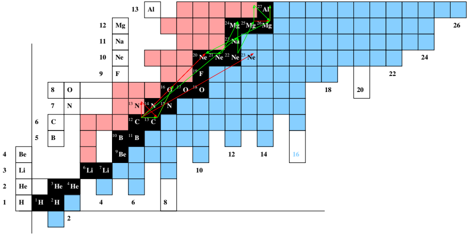

from A. Chieffi *et al.*, APJ **502** (1998), 737

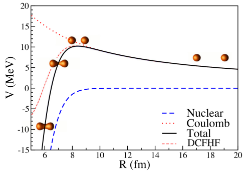

C. Simenel *et al.*, Prog Part Nucl Phys **103** (2018), 19

Heavy ion reactions during carbon burning in massive stars

- $M \geq 7.5 \ldots 9.5\, M_{\odot}$
- core made of oxygen and carbon
- Coulomb well

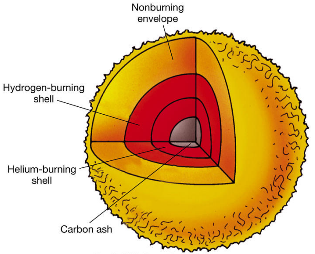

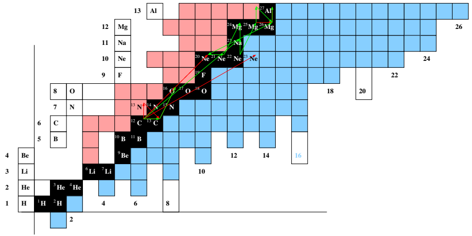

from A. Chieffi *et al.*, APJ **502** (1998), 737

$$^{12}\mathrm{C} + ^{12}\mathrm{C} \rightarrow ^{24}\mathrm{Mg}^* \rightarrow ^{24}\mathrm{Mg} + \gamma$$
$$\rightarrow ^{20}\mathrm{Ne} + \alpha$$
$$\rightarrow ^{23}\mathrm{Na} + \mathrm{p}$$
$$\rightarrow ^{23}\mathrm{Mg} + \mathrm{n}$$

Exit channels of light fusing systems: $^{12}C+^{12}C$

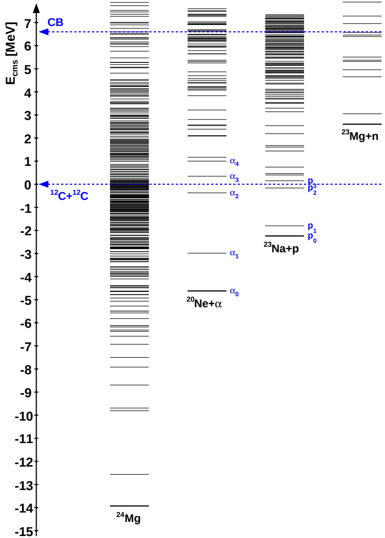

- *Q – value*

- measure particles
- measure gammas cascades!

- ground state: α_0, p_0, *etc.*
- excited states: $\alpha_0, \alpha_1, \alpha_3, ..$

- ^{24}Mg: compound nucleus from $^{12}C+^{12}C$ fusion of 0^+ particles

https://www.nndc.bnl.gov

Exit channels of light fusing systems: $^{12}C + ^{12}C$

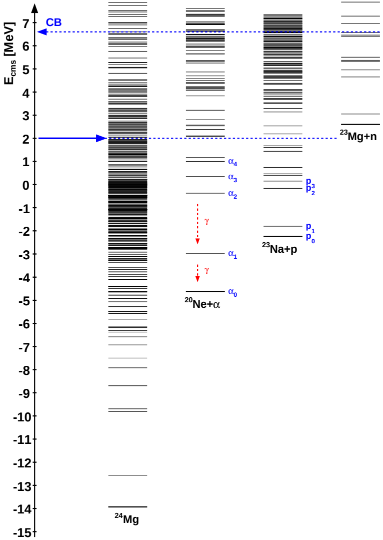

https://www.nndc.bnl.gov

- *Q – value*
- measure particles
- measure gammas cascades!
- ground state: α_0, p_0, *etc.*
- excited states: $\alpha_0, \alpha_1, \alpha_3, ..$
- ^{24}Mg: compound nucleus from $^{12}C + ^{12}C$ fusion of 0^+ particles

Exit channels of light fusing systems: $^{12}C+^{12}C$

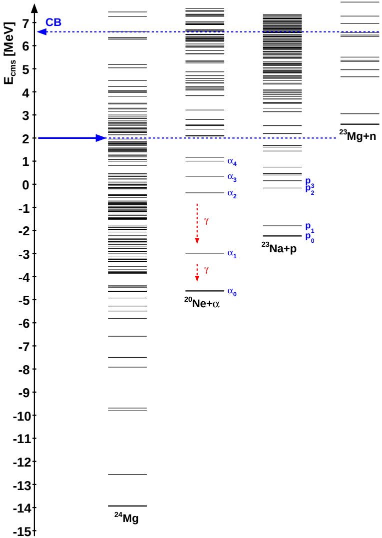

https://www.nndc.bnl.gov

- *Q – value*
- measure particles
- measure gammas cascades!
- ground state: α_0, p_0, *etc.*
- excited states: $\alpha_0, \alpha_1, \alpha_3, ..$
- ^{24}Mg: compound nucleus from $^{12}C+^{12}C$ fusion of 0^+ particles (evaluated) positive even parity states

Exit channels of light fusing systems: $^{12}C+^{12}C$

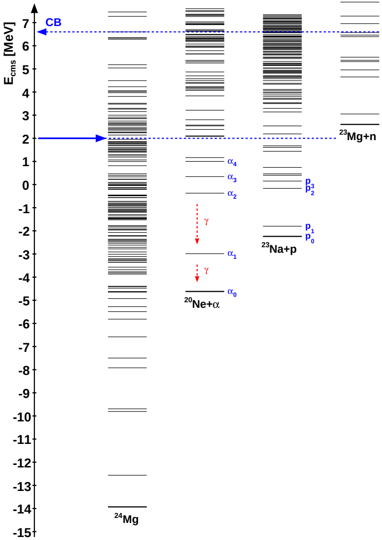

- ^{24}Mg: compound nucleus from $^{12}C+^{12}C$
  fusion of 0^+ particles
  (evaluated) positive even parity states

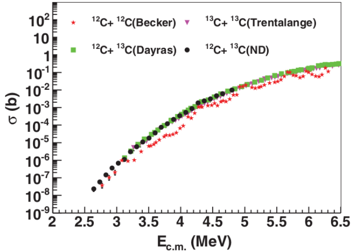

M. Notani *et al.*, PRC **85** (2012), 014607

https://www.nndc.bnl.gov

Exit channels of light fusing systems: $^{12}C+^{12}C$

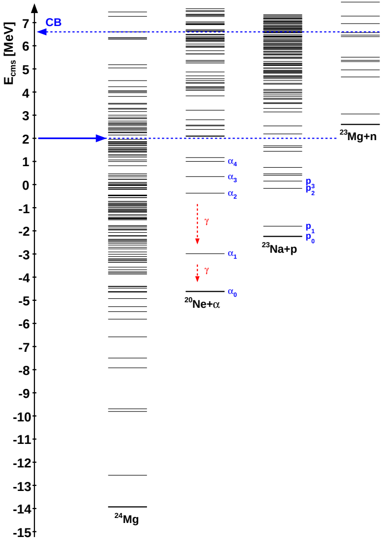

- ^{24}Mg: compound nucleus from $^{12}C+^{12}C$
  fusion of 0^+ particles
  (evaluated) positive even parity states

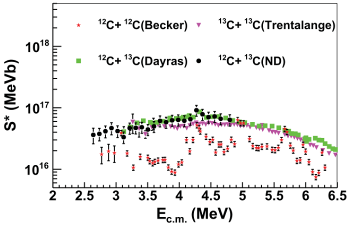

M. Notani *et al.*, PRC **85** (2012), 014607

https://www.nndc.bnl.gov

Angular momentum conservation and angular distributions

N. Bohr hypothesis of independence: compound formation and decay are independent
but angular momentum conservation

fusion of spinless particles:

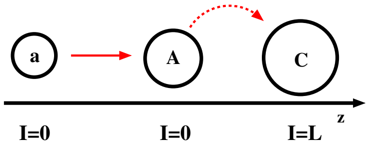

- L perpendicular to z
- equal probability $\pm$ z

$$\left(\frac{d\sigma}{d\Omega}\right) = \sum_{k=0}^{k_{max}} a_k P_k(\cos(\theta)),\ k = 0, 2, 4, ..$$

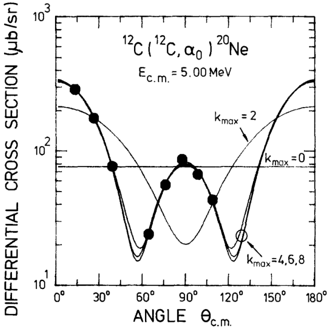

Angular momentum conservation and angular distributions

N. Bohr hypothesis of independence: compound formation and decay are independent

but angular momentum conservation

fusion of spinless particles:

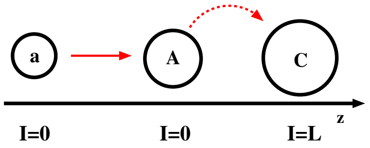

- L perpendicular to z
- equal probability ± z

$$\left(\frac{d\sigma}{d\Omega}\right) = \sum_{k=0}^{k_{max}} a_k P_k(\cos(\theta)),\ k = 0, 2, 4, ..$$

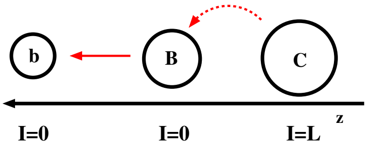

→ compound state spin from fusion measurements

- normalisation of cross sections: $P_0(\cos(\theta))$

Fusion formation and population of compound states

identical 0^+ particles:

$$^{12}\mathrm{C} + ^{12}\mathrm{C} \rightarrow {}^{24}\mathrm{Mg}^*$$
$$0^+ + 0^+ \rightarrow \quad ??$$

wave function:

$$|\Psi\rangle = |\Phi\rangle_{\mathrm{space}} \otimes |\Phi\rangle_{\mathrm{spin}} \otimes |\Phi\rangle_{\mathrm{isospin}}$$
$$|\Phi\rangle_{\mathrm{space}} = R_n(r) Y_l^m(\theta, \phi)$$
$$Y_l^m(\pi - \theta, \phi + \pi) = -1^l Y_l^m(\theta, \phi)$$
$$\rightarrow l = 0, 2, 4, ..$$

parity is multiplicative:

$$P_{\mathrm{Mg}} = -1^l P_{\mathrm{C}} \cdot P_{\mathrm{C}}$$

Fusion formation and population of compound states

identical 0^+ particles:

$$^{12}\mathrm{C} + ^{12}\mathrm{C} \rightarrow ^{24}\mathrm{Mg}^*$$

$$0^+ + 0^+ \rightarrow \quad ??$$

wave function:

$$|\Psi\rangle = |\Phi\rangle_{\mathrm{space}} \otimes |\Phi\rangle_{\mathrm{spin}} \otimes |\Phi\rangle_{\mathrm{isospin}}$$

$$|\Phi\rangle_{\mathrm{space}} = R_n(r)\, Y_l^m(\theta, \phi)$$

$$Y_l^m(\pi - \theta, \phi + \pi) = -1^l\, Y_l^m(\theta, \phi)$$

$$\rightarrow l = 0, 2, 4, ..$$

parity is multiplicative:

$$P_{\mathrm{Mg}} = -1^l\, P_{\mathrm{C}} \cdot P_{\mathrm{C}}$$

This work			Previous work				
E (MeV)	Γ_{el} (keV)	Γ_{tot} (keV)	l	E (MeV)	Γ_{el} (keV)	Γ_{tot} (keV)	Ref.
4.25	0.4	80	0	4.25		60–80	[3]
(5.71)	35	70	(0)				[3]
5.80	2.37	50	0	5.82		50	[13]
5.97	9.0	50	0	5.97		50	[13]
4.64	0.04	40	2	4.62		60–80	[3]
4.865	1.0	80	2	4.88		80	[3]
4.99	2.0	100	2	5.00		60–80	[3]
5.38	1.4	80	2	5.37		60–80	[3]
5.66	6.0	50	2	5.64		140	[3]
			2	5.6	20	104	[54]
			2	5.6	10	130	[55]
5.78	0.38	60	2	5.8		60	[13]
6.01	6.2	50	2	6.01		70	[13]
6.29	15	60	2	6.25		60–80	[3]
				6.28	⩾16	125	[7]
6.65	11	50	2	6.64	29	100	[55]
				6.63	40	100	[7]
4.44		60	4	4.46		60–80	[3]
	0.045						
5.75	0.06	60	4	5.77		60	[13]
5.95	1.5	50	4	5.92	4	60	[3]
				5.96	⩾3	100	[7]
			4	5.94		50	[13]
					3.75		
			4	6.0	7.5	88	[54]
			4	6.0	4	100	[55]
6.49	0.4	50	(6)	6.49		⩾50	[7]

E.F. Aguilera *et al.*, PRC **73** (2006), 064601

Fusion formation and population of compound states

identical 0^+ particles:

$$^{12}\mathrm{C} + ^{12}\mathrm{C} \rightarrow ^{24}\mathrm{Mg}^*$$

$$0^+ + 0^+ \rightarrow \quad ??$$

wave function:

$$|\Psi\rangle = |\Phi\rangle_{\mathrm{space}} \otimes |\Phi\rangle_{\mathrm{spin}} \otimes |\Phi\rangle_{\mathrm{isospin}}$$

$$|\Phi\rangle_{\mathrm{space}} = R_n(r)\, Y_l^m(\theta, \phi)$$

$$Y_l^m(\pi - \theta, \phi + \pi) = -1^l\, Y_l^m(\theta, \phi)$$

$$\rightarrow l = 0, 2, 4, ..$$

parity is multiplicative:

$$P_{\mathrm{Mg}} = -1^l\, P_{\mathrm{C}} \cdot P_{\mathrm{C}}$$

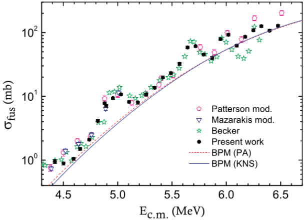

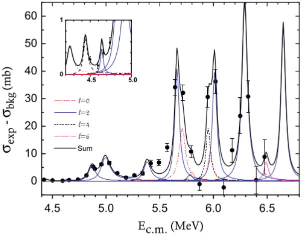

E.F. Aguilera *et al.*, PRC **73** (2006), 064601

Typical fusion excitation function into low-count acquisition runs

sub barrier $^{12}C+^{12}C$:

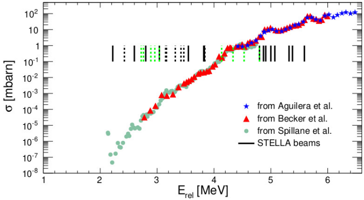

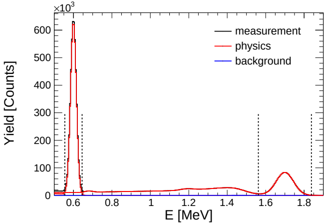

Typical fusion excitation function into low-count acquisition runs

sub barrier $^{12}C+^{12}C$:

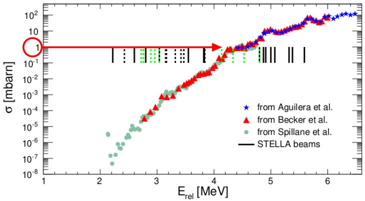

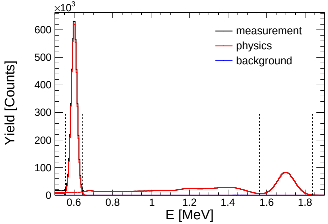

- physics: 0.6 MeV, 1.7 MeV

  well defined peaks, $\pm 3\sigma$ gates

Typical fusion excitation function into low-count acquisition runs

sub barrier $^{12}C+^{12}C$:

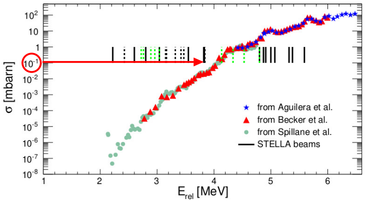

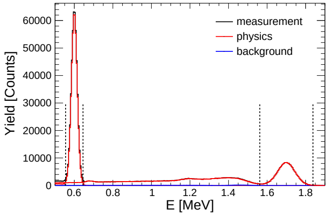

- physics: 0.6 MeV, 1.7 MeV
  well defined peaks, $\pm 3\sigma$ gates

Typical fusion excitation function into low-count acquisition runs

sub barrier $^{12}C+^{12}C$:

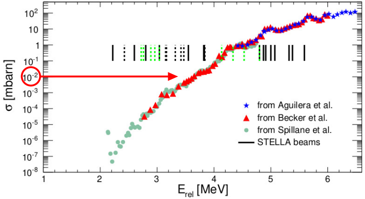

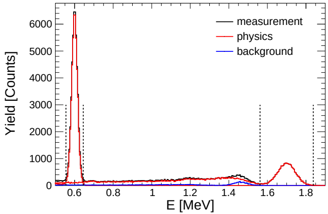

- physics: 0.6 MeV, 1.7 MeV
  well defined peaks, $\pm 3\sigma$ gates
- background: 1.46 MeV
  background model: linear, exponential

Typical fusion excitation function into low-count acquisition runs

sub barrier $^{12}C+^{12}C$:

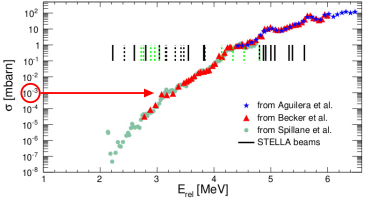

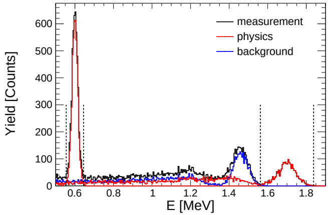

- physics: 0.6 MeV, 1.7 MeV
  well defined peaks, $\pm 3\sigma$ gates
- background: 1.46 MeV
  background model: linear, exponential

Typical fusion excitation function into low-count acquisition runs

sub barrier $^{12}C+^{12}C$:

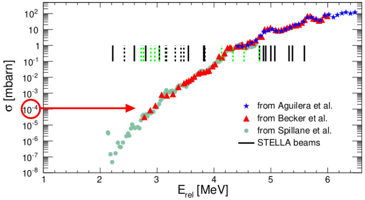

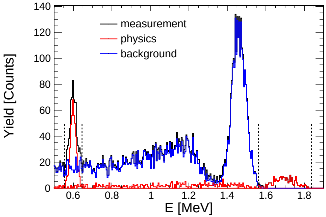

- physics: 0.6 MeV, 1.7 MeV
  well defined peaks, $\pm 3\sigma$ gates
- background: 1.46 MeV
  background model: linear, exponential

Typical fusion excitation function into low-count acquisition runs

sub barrier $^{12}C+^{12}C$:

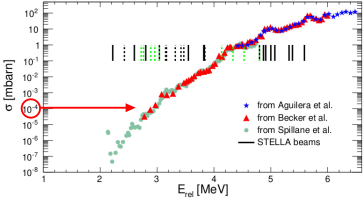

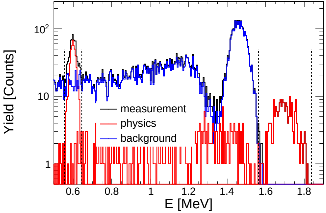

- physics: 0.6 MeV, 1.7 MeV
  well defined peaks, $\pm 3\sigma$ gates
- background: 1.46 MeV
  background model: linear, exponential
- statistical uncertainty
- tails of background contributions

Typical fusion excitation function into low-count acquisition runs

sub barrier $^{12}C+^{12}C$:

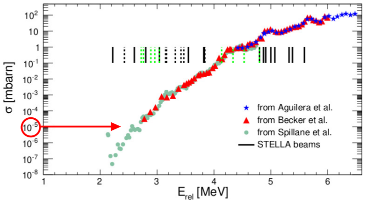

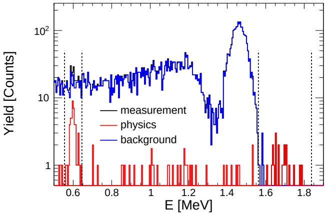

- physics: 0.6 MeV, 1.7 MeV

  well defined peaks, $\pm 3\sigma$ gates
- background: 1.46 MeV

  background model: linear, exponential

- statistical uncertainty
- tails of background contributions

Typical fusion excitation function into low-count acquisition runs

sub barrier $^{12}C+^{12}C$:

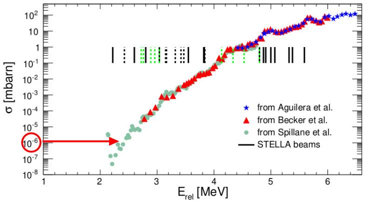

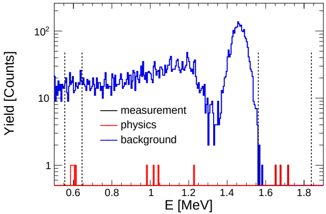

- physics: 0.6 MeV, 1.7 MeV
  well defined peaks, $\pm 3\sigma$ gates
- background: 1.46 MeV
  background model: linear, exponential

- statistical uncertainty
- tails of background contributions

sub nano barn cross sections:

- few counts statistic
- background fluctuations

astrophysics region of interest:

- 8..10 $M_\odot$: 1.5 ± 0.3 MeV
- 25 $M_\odot$: 2.25 ± 0.5 MeV

$$S^* = \sigma(E)E \cdot \exp(2\pi\eta + gE)$$

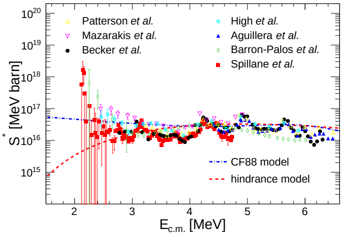

- strong fluctuations of the excitation function
  - → increase of reaction rate
  - extrapolations uncertain
  - experimental resolution needed
- possible fusion hindrance with broad maximum
  - → ceasing of reaction rate
  - ? phenomenological model suited
- low cross sections of stiff nuclei
  - → decrease of reaction rate
  - beam intensities of a few pµA
  - data taking of weeks
  - background suppression
  - low count statistics

astrophysics region of interest:

- 8..10 $M_\odot$: 1.5 ± 0.3 MeV
- 25 $M_\odot$: 2.25 ± 0.5 MeV

- strong fluctuations of the excitation function
  - → increase of reaction rate
  - extrapolations uncertain
  - experimental resolution needed
- possible fusion hindrance with broad maximum
  - → ceasing of reaction rate
  - ? phenomenological model suited
- low cross sections of stiff nuclei
  - → gamma-particle coincidences
  - beam intensities of a few pμA
  - data taking of weeks
  - background suppression
  - low count statistics

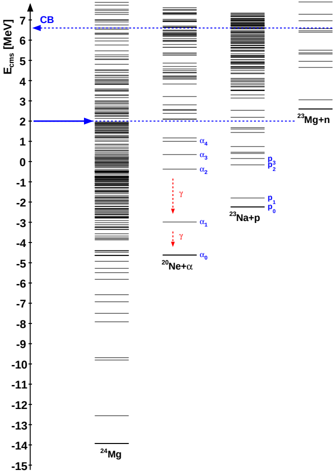

astrophysics region of interest:

- 8..10 $M_\odot$: 1.5 ± 0.3 MeV
- 25 $M_\odot$: 2.25 ± 0.5 MeV

- strong fluctuations of the excitation function
  - → increase of reaction rate
  - extrapolations uncertain
  - experimental resolution needed
- possible fusion hindrance with broad maximum
  - → ceasing of reaction rate
  - ? phenomenological model suited
- low cross sections of stiff nuclei
  - → gamma-particle coincidences
  - beam intensities of a few pμA
  - data taking of weeks
  - background suppression
  - low count statistics

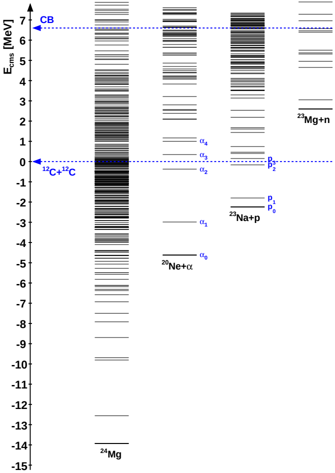

Cluster States from ^{24}Mg(α, α')^{24}Mg

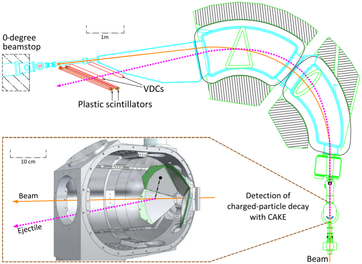

P. Adsley *et al.*, PRL **129** (2022), 102701

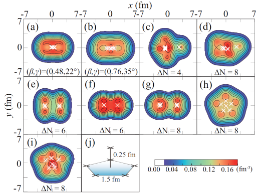

Y. Chiba and M. Kimura, PRC **91** (2015), 061302(R)

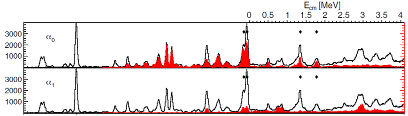

P. Adsley *et al.*, PRL **129** (2022), 102701

- 0^+ states at reaction thresholds
- 0^+_5 and 0^+_8 cluster configurations
- extreme α/p decay branching

“[..] we must still realise that the subsequent escape of α-rays or protons necessitates a separate *concentration process* for the excess energy and that in particular we cannot draw any decisive conclusion from these phenomena about the presence of such particles in nuclei under normal conditions.”

N. Bohr, Nature **137** (1936), 344

astrophysics region of interest:

- 8..10 $M_\odot$: 1.5 ± 0.3 MeV
- 25 $M_\odot$: 2.25 ± 0.5 MeV

- strong fluctuations of the excitation function
  - → increase of reaction rate
  - extrapolations uncertain
  - experimental resolution needed
- possible fusion hindrance with broad maximum
  - → ceasing of reaction rate
  - ? phenomenological model suited
- low cross sections of stiff nuclei
  - → gamma-particle coincidences
  - beam intensities of a few pμA
  - data taking of weeks
  - background suppression
  - low count statistics

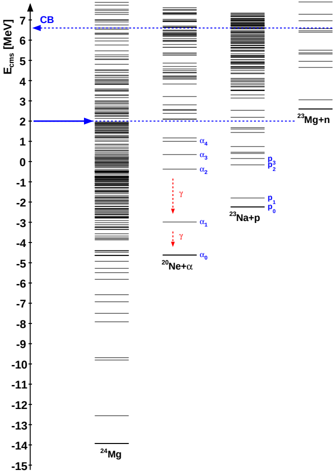

$$^{12}\mathrm{C} + ^{12}\mathrm{C} \rightarrow ^{23}\mathrm{Na}^{*} + \mathrm{p}$$
$$\rightarrow ^{20}\mathrm{Ne}^{*} + \alpha$$

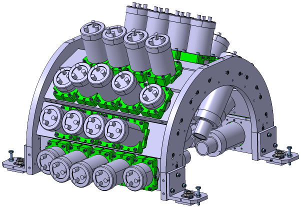

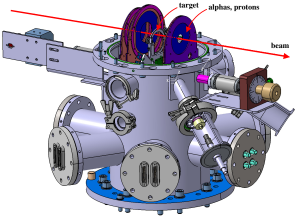

courtesy G. Heitz

- ^{12}C beam intensities of a few pμA
  30. . . 50 μg/cm^2 self supporting ^{12}C foil

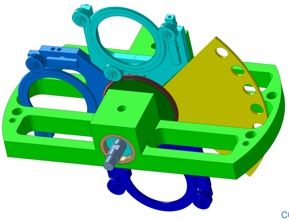

courtesy M. Krauth

- in/off-beam intensity monitoring
- offline target thickness scans
- carbon morphology: Raman spectroscopy

$$^{12}\mathrm{C} + ^{12}\mathrm{C} \rightarrow ^{23}\mathrm{Na}^* + \mathrm{p}$$
$$\rightarrow ^{20}\mathrm{Ne}^* + \alpha$$

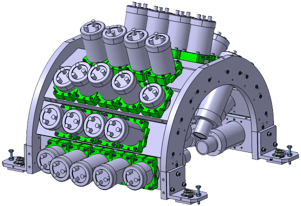

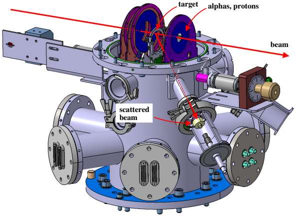

courtesy G. Heitz

- ^{12}C beam intensities of a few pμA
  30…50 μg/cm^2 self supporting ^{12}C foil

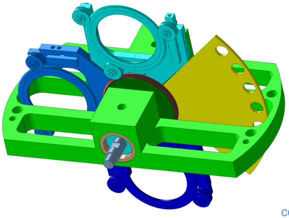

courtesy M. Krauth

- in/off-beam intensity monitoring
- offline target thickness scans
- carbon morphology: Raman spectroscopy

$$^{12}\mathrm{C} + ^{12}\mathrm{C} \rightarrow ^{23}\mathrm{Na}^* + \mathrm{p}$$
$$\rightarrow ^{20}\mathrm{Ne}^* + \alpha$$

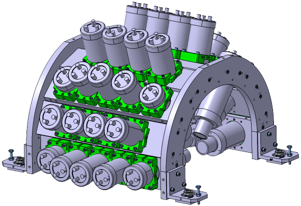

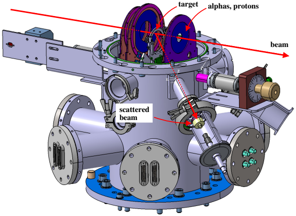

courtesy G. Heitz

- ^{12}C beam intensities of a few pμA
  30. . . 50 μg/cm^2 self supporting ^{12}C foil
- fast-timing measurements
  synchronization of DAQ's:
  1 GHz gamma (UK-FATIMA)
  125 MHz particle (STELLA)
- monitor and correct time drift:

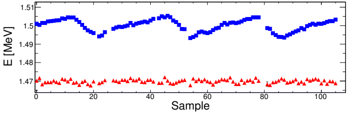

M. Heine *et al.*, NIM A **903** (2018), 1

Target stability with long data acquisition runs

1. thickness from weighting upon production
2. monitoring of ratio: beam scattering detector and beam integrator
3. Raman scattering analysis of material (on and off beam spot)
   G. Fruet *et al.*, PRL **124** (2020), 192701

   thickness from alpha particle energy loss (on and off beam spot)

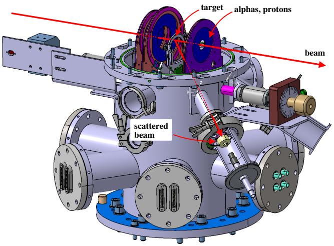

courtesy G. Heitz

Target stability with long data acquisition runs

1. thickness from weighting upon production
2. monitoring of ratio: beam scattering detector and beam integrator
3. Raman scattering analysis of material (on and off beam spot)
   G. Fruet *et al.*, PRL **124** (2020), 192701

   thickness from alpha particle energy loss (on and off beam spot)

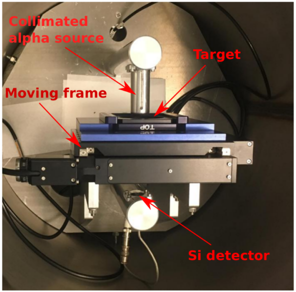

courtesy J. Nippert

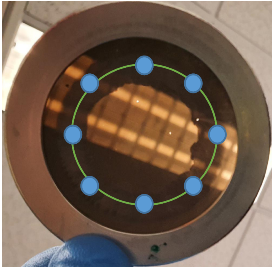

J. Nippert *et al.*, Acta Phys Pol B Proc Suppl **17** (2024), 3-A33

Target stability with long data acquisition runs

1. thickness from weighting upon production
2. monitoring of ratio: beam scattering detector and beam integrator
3. Raman scattering analysis of material (on and off beam spot)
   G. Fruet *et al.*, PRL **124** (2020), 192701

   thickness from alpha particle energy loss (on and off beam spot)

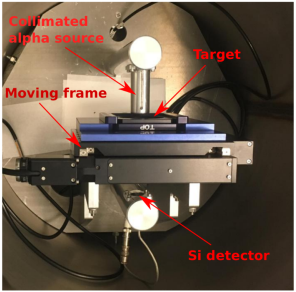

courtesy J. Nippert

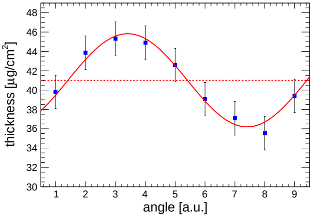

J. Nippert *et al.*, Acta Phys Pol B Proc Suppl **17** (2024), 3-A33

Target stability with long data acquisition runs

1. thickness from weighting upon production
2. monitoring of ratio: beam scattering detector and beam integrator
3. Raman scattering analysis of material (on and off beam spot)
   G. Fruet *et al.*, PRL **124** (2020), 192701

   thickness from alpha particle energy loss (on and off beam spot)

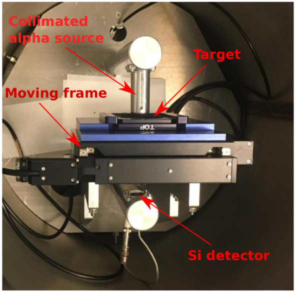

courtesy J. Nippert

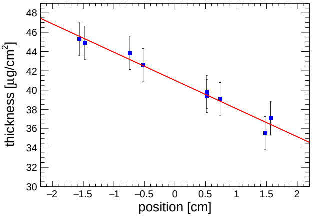

J. Nippert *et al.*, Acta Phys Pol B Proc Suppl **17** (2024), 3-A33

Background dominated data acquisition rates

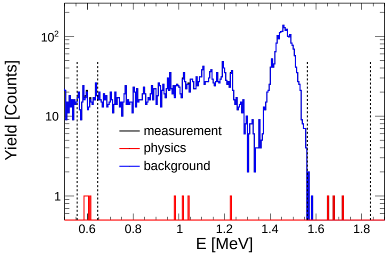

- n : measurement
- μ: physics
- b: background

- R_γ, R_p: acquisition rates

$$b = R_\gamma \cdot R_\text{p} \cdot t_\text{coinc} \cdot t_\text{acqu}$$
$$\mu = n - b$$

- determination of rates in gamma and particle detectors independently

C.L. Jiang *et al.*, PRC **97** (2018), 012801(R)

“Conventional” background estimation

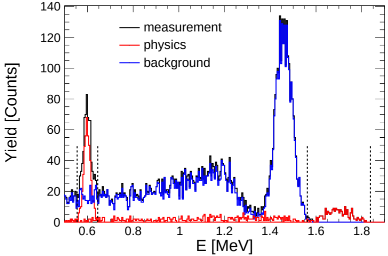

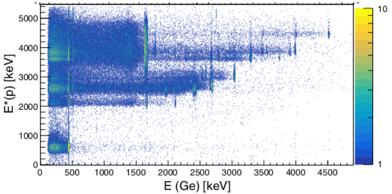

- estimate background (linear, exponential) just outside energy selection gates
- generalise for 2D spectra
- W.P. Tan *et al.*, PRL **124** (2020), 192702

“Conventional” background estimation

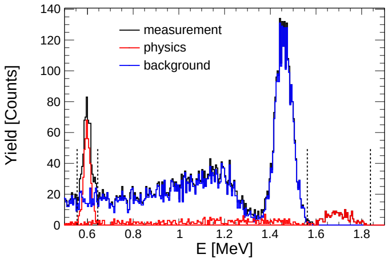

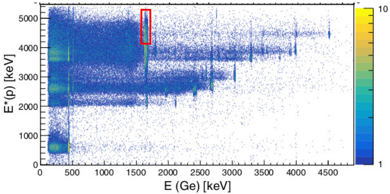

- estimate background (linear, exponential) just outside energy selection gates
- generalise for 2D spectra
- W.P. Tan *et al.*, PRL **124** (2020), 192702

Fast timing background estimation with STELLA

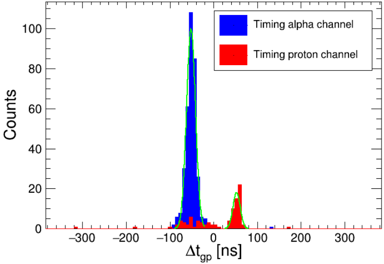

J. Nippert *et al.*, submitted to PRC

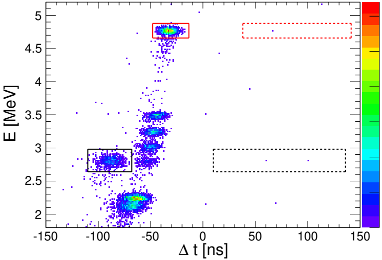

M. Heine *et al.*, EPJ Web Conf **260** (2022), 01004

- identical energy gates for gammas and particles
- select background in non coincident timing domain
- $\sim$ 10 ns gamma-particle timing gates
- G. Fruet *et al.*, PRL **124** (2020), 192701

Statistical significance in low count-rate measurements

- estimate confidence interval of a signal μ in a measurement n with background b
  $\mu = n - b$
- avoid negative signals (nonphysical)
- limits and asymmetric error bars

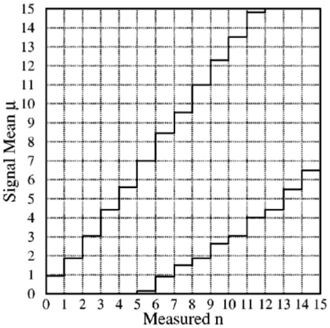

G.J. Feldman and R.D. Cousins *et al.*, PRD **57** (1998), 3873

n	b	μ	$\Delta\mu$	$\Delta\mu_{\mathrm{FC}}$
15	12	3	$\sqrt{27}$	[0, 6.32]
1	1	0	$\sqrt{2}$	[0, 1.75]
2	2	0	$\sqrt{4}$	[0, 2.25]

Background reduction with STELLA and exclusive exit channels

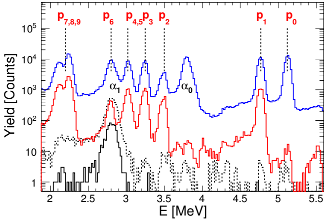

M. Heine *et al.*, NIM A **903** (2018), 1

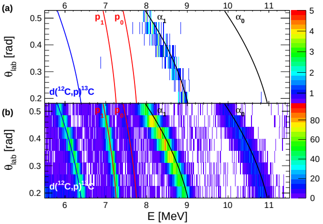

G. Fruet *et al.*, PRL **124** (2020), 192701

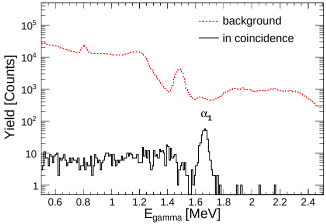

G. Fruet *et al.*, PRL **124** (2020), 192701

- identical energy gates for gammas and particles
- select background in non coincident timing domain
- $\sim$ 10 ns gamma-particle timing gates

$$S^* = \sigma(E)E \cdot \exp(2\pi\eta + gE)$$

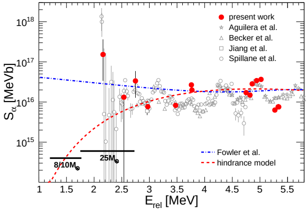

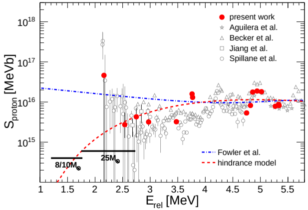

G. Fruet *et al.*, PRL **124** (2020), 192701

α_1 S^*-factor (coincidences)

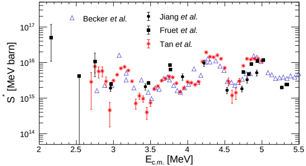

p_1 S^*-factor (coincidences)

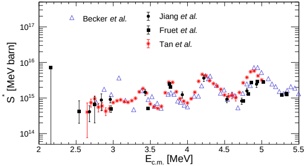

Target thickness and effective beam energy

- beam undergoes energy loss in thin target foil: $\mathcal{O}$ (100 keV)
- nominal energy of evaporated alphas and protons
- correction for foil protecting detector

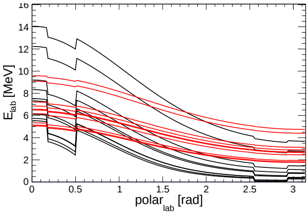

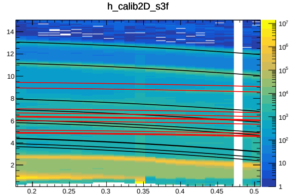

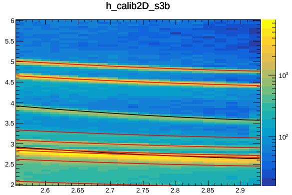

↪ quite sensitive to beam energy

match to experimental data:

- 24 angles per detector

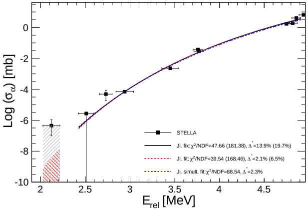

- fit alphas and protons simultaneously
- Hin: hindrance model (free) parameters:
  C.L. Jiang *et al.* PRC **75**, (2007) 015803
- HinRes: hindrance plus resonance from:
  T. Spillane *et al.* PRL **98**, (2007) 122501
- 2.5...4.0 MeV: observation of hindrance
- $\leq$ 2.5 MeV: change of mechanism?

$$\mathrm{a} + \mathrm{A} \rightarrow \mathrm{b} + \mathrm{B}$$

$$\lambda = N_a N_A \langle v \cdot \sigma(v) \rangle$$

velocity/energy distribution:

$$\Phi = \sqrt{\frac{8m}{\pi (k_\mathrm{B} T)^2}} E \exp(-E/k_\mathrm{B} T)$$

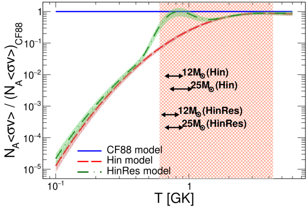

E. Monpribat *et al.*, A&A **660**, (2022) A47

Modelling of the cross section and reaction rates

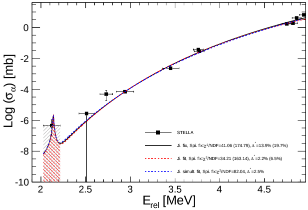

- fit alphas and protons simultaneously
- Hin: hindrance model (free) parameters:
  C.L. Jiang *et al.* PRC **75**, (2007) 015803
- HinRes: hindrance plus resonance from:
  T. Spillane *et al.* PRL **98**, (2007) 122501
- 2.5...4.0 MeV: observation of hindrance
- $\leq$ 2.5 MeV: change of mechanism?

$$\mathrm{a} + \mathrm{A} \rightarrow \mathrm{b} + \mathrm{B}$$

$$\lambda = N_a N_A \langle v \cdot \sigma(v) \rangle$$

velocity/energy distribution:

$$\Phi = \sqrt{\frac{8m}{\pi (k_\mathrm{B} T)^2}} E \exp(-E/k_\mathrm{B} T)$$

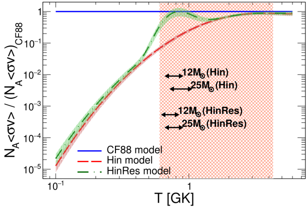

E. Monpribat *et al.*, A&A **660**, (2022) A47

Modelling of the cross section and reaction rates

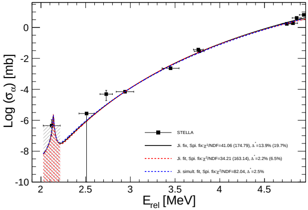

- fit alphas and protons simultaneously
- Hin: hindrance model (free) parameters:
  C.L. Jiang *et al.* PRC **75**, (2007) 015803
- HinRes: hindrance plus resonance from:
  T. Spillane *et al.* PRL **98**, (2007) 122501
- 2.5...4.0 MeV: observation of hindrance
- $\leq$ 2.5 MeV: change of mechanism?

$$\mathrm{a} + \mathrm{A} \rightarrow \mathrm{b} + \mathrm{B}$$

$$\lambda = N_a N_A \langle v \cdot \sigma(v) \rangle$$

velocity/energy distribution:

$$\Phi = \sqrt{\frac{8m}{\pi (k_\mathrm{B} T)^2}} E \exp(-E/k_\mathrm{B} T)$$

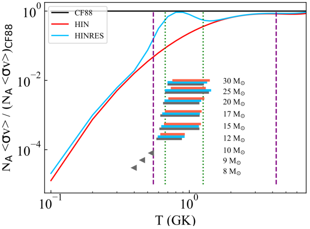

T. Dumont *et al.*, A&A **688**, (2024) A115

Summary and outlook

- carbon fusion in quiescent burning
- ultra low cross sections in astrophysics region of interest

- background suppression with coincidence method
  - UniStra IdEX project STELLA (STELlar LAboratory) developed at IPHC
  - collaboration with UK-FATIMA ($LaBr_3Ce$ detectors)
  - fast timing for background reduction
  - exclusive $^{12}C+^{12}C$ cross sections in the astrophysics region of interest

- modelling of response function (Hin and HinRes)
- translation of measured cms energies into temperature regime
- comparison to effective carbon core temperatures in stellar burning

- underground experiment for superior background reduction
- $^{12}C+^{16}O$ and $^{16}O+^{16}O$ at Andromède, Orsay

Thank you for your attention!